ChemComm

COMMUNICATION

View Article Online
View Journal | View Issue

Cite this: *Chem. Commun.*, 2014, **50**, 12465

Received 16th July 2014,
Accepted 22nd August 2014

DOI: 10.1039/c4cc05478d

www.rsc.org/chemcomm

Spatial co-localization of multi-enzymes by inorganic nanocrystal–protein complexes†

Zhixian Li,[a] Yifei Zhang,[a] Yechao Su,[a] Pingkai Ouyang,[b] Jun Ge*[a] and Zheng Liu*[a]

We report a simple precipitation method for the construction of spatially co-localized multi-enzyme systems based on inorganic nanocrystal–protein complexes. A spatially controlled multi-enzyme system exhibits enhanced overall catalytic performance, allowing for sensitive detection of glucose in solution.

Compartmentalization is the key to achieve high efficiency of biological reactions in living cells, where precisely co-localized multiple enzymes catalyze various multi-step cascade reactions. This compartmentalization *in vivo* inspires the construction of artificial multi-enzyme systems enabling many promising applications.[1–3] Co-immobilization of enzymes on polymeric capsules,[4,5] DNA scaffolds,[6–10] protein scaffolds,[11,12] and other systems[13–17] has been proven to be effective for constructing complex multi-enzyme systems. However, a robust and easy-to-use method for fabricating spatially co-localized multi-enzyme systems with high catalytic efficiency has remained a challenge. In this study, we present a simple method that produces multi-enzyme–inorganic nanocrystal complexes with pre-defined spatial co-localization of enzymes, mimicking *in vivo* compartmentalization. We demonstrate that the spatially controlled co-localization of enzymes plays a crucial role in the overall enzyme activity enhancement of the artificial multi-enzyme system.

Recently, Ge *et al.*[18] and Zeng and co-workers[19] reported a method of preparing enzyme–inorganic nanocrystal complexes with flower-like shapes by simply adding metal ions to the protein solution in phosphate buffer. Protein molecules were complexed with copper phosphate nanocrystals and served as 'glue' to bind the nanocrystals together to form the protein–inorganic hybrid nanoflowers.[18] In the present study, we extended the above mentioned co-precipitation method to construct multi-enzyme complexes. As shown in Scheme 1, by this simple method, the spatial co-localization of enzymes can be conveniently achieved.

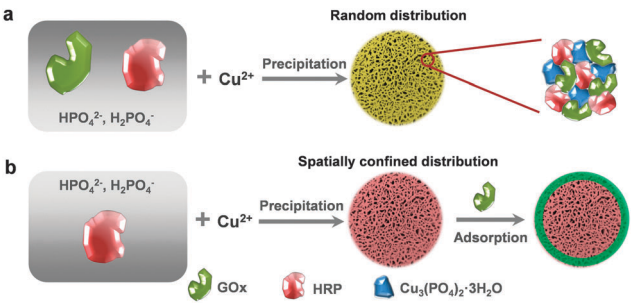

Scheme 1 Schematic illustration of the preparation of multi-enzyme incorporated complexes. (a) Randomly distributed multi-enzyme complexes as a control; (b) spatially co-localized multi-enzyme complexes.

We chose horseradish peroxidase (HRP) and glucose oxidase (GOx) as the model enzymes for a cascade reaction. In the synthesis of spatially co-localized multi-enzyme complexes, as shown in Scheme 1b, 50 mL of phosphate buffer saline solution (PBS, 10 mM, pH 7.4) containing 0.25 mg mL^{-1} of HRP was first mixed with 1.5 mL of $CuSO_4$ in water solution (200 mM) at 4 °C for 24 h to form the HRP-incorporated complexes. Then, the HRP-incorporated complexes were incubated in another PBS solution containing 0.25 mg mL^{-1} of GOx for another 24 h at 4 °C to adsorb the second enzyme on the surface of the complexes by the coordination interaction between Cu^{2+} and amino acids of proteins. Then the GOx@HRP complexes (GOx@HRP) were obtained after centrifugation and washed with deionized water to remove the loosely adsorbed proteins. To examine the compartmentalization effect, the above mentioned method was also applied to synthesize HRP@GOx in which GOx was used in the first step, HRP in the second. Randomly distributed multi-enzyme complexes (GOx–HRP) were prepared as the control (Scheme 1a), in which 50 mL of phosphate buffer saline (PBS, 10 mM, pH 7.4) solution containing 0.25 mg mL^{-1} of GOx and 0.25 mg mL^{-1} of HRP was mixed with 1.5 mL of $CuSO_4$ in water solution (200 mM), followed by a stationary incubation for 24 h at 4 °C.

[a] *Key Lab for Industrial Biocatalysis, Ministry of Education, Department of Chemical Engineering, Tsinghua University, Beijing 100084, China. E-mail: junge@mail.tsinghua.edu.cn*
[b] *College of Biotechnology and Pharmaceutical Engineering, Nanjing University of Technology, Nanjing 211816, China*

† Electronic supplementary information (ESI) available. See DOI: 10.1039/c4cc05478d

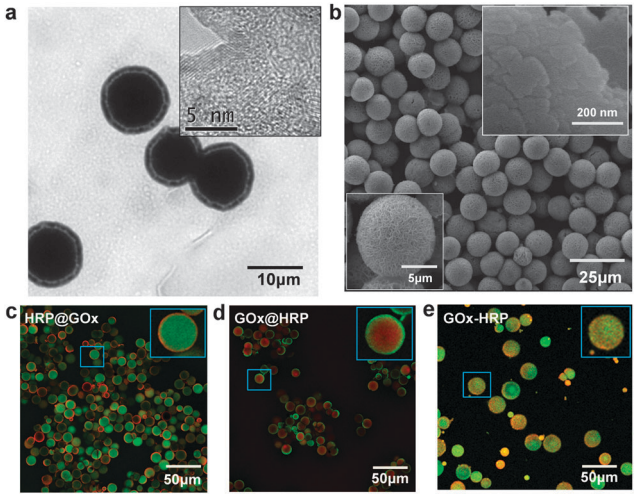

Fig. 1 Structural characterizations of multi-enzyme incorporated complexes. (a) A typical transmission electron microscopy (TEM) image of GOx@HRP (inset: high-resolution TEM of one petal); (b) a typical scanning electron microscopy (SEM) image of GOx@HRP (inset: high-resolution SEM of petals); (c)–(e) confocal microscopy images of (c) HRP@GOx, (d) GOx@HRP, and (e) GOx–HRP (HRP and GOx were labeled with RhB (red) and FITC (green), respectively).

Fig. 1a and b show the transmission electron microscopy (TEM) and scanning electron microscopy (SEM) images of the complexes containing HRP and GOx. The high-resolution TEM image of one petal of the complex shows the crystal structure of the complex (Fig. 1a inset). The complexes have an average size of ~10 μm with highly porous structures (Fig. 1b). The high-resolution SEM image of the petals shows that the complex is formed by the stacked nanocrystals (Fig. 1b inset). The powder X-ray diffraction pattern of the multi-enzyme incorporated complexes fits that of $Cu_3(PO_4)_2{\cdot}3H_2O$ (Fig. S1a, ESI†), which agrees well with the results of our previous study.[18] As we discussed in our previous study,[18] proteins induce the crystallization of $Cu_3(PO_4)_2{\cdot}3H_2O$ and bind the nanocrystals together to assemble into flower-like structures. To investigate the spatial distribution of enzymes, GOx and HRP were labeled with fluorescent probes fluorescein isothiocyanate (FITC) and rhodamine B (RhB), respectively. The multi-enzyme complexes were observed under a confocal microscope. Core–shell structures are clearly observed for both HRP@GOx (Fig. 1c) and GOx@HRP (Fig. 1d). And the Z-stack confocal images of GOx@HRP further confirmed the structures (Fig. S2 and Movie S1, ESI†). In contrast, GOx–HRP (Fig. 1e) appears to have a random distribution of HRP and GOx molecules.

The total enzyme loadings for all the three types of multi-enzyme incorporated complexes were around 10 wt%, calculated by measuring the protein concentration in solution using a standard BCA method. Furthermore, we confirmed the incorporation of enzymes by the thermal gravimetric analysis (TGA). For GOx@HRP (Fig. S1e, ESI†), the first-stage decomposition of the hybrid complexes in air starts from 25 °C and finishes around 200 °C, caused by the removal of physically adsorbed and bound water molecules. The decomposition of enzymes starts at around 200–300 °C, which is much lower than the decomposition temperature of the inorganic components (600 °C). During this stage, the total weight loss is around 10%, confirming that the total weight percentage of proteins loaded in complexes is approximately 10 wt%, agreeing well with the BCA protein concentration measurements. However, the individual weight percentage of GOx and HRP loaded onto the three complexes were varied. For GOx–HRP, the content of HRP was calculated by UV absorption at 403 nm, while the total protein content was calculated by the BCA assay. For GOx@HRP and HRP@GOx, the content of GOx and HRP was determined by the BCA assay in each step of the preparation. The loading amounts of GOx and HRP in GOx@HRP, HRP@GOx and GOx–HRP were (2 wt%, 8 wt%), (8 wt%, 2 wt%) and (5 wt%, 5 wt%), respectively.

The overall enzymatic activities of GOx@HRP, HRP@GOx, and GOx–HRP at the same total protein content were measured using 20 mM glucose and 1 mM ABTS as the substrates in PBS solution (Fig. 2a). The free GOx and HRP systems in solution with the same protein amount and the corresponding GOx and HRP ratios were utilized as controls. As shown in Fig. 2b, compared to the free enzyme systems, all the three types of multi-enzyme complexes showed increased overall enzymatic activity (140–310%). Obvious activity loss often occurs during enzyme immobilization or encapsulation, which is caused by either denaturation of the enzymes or hindered mass transfer within the solid carriers. A nanoscale matrix offers a way to reduce the mass

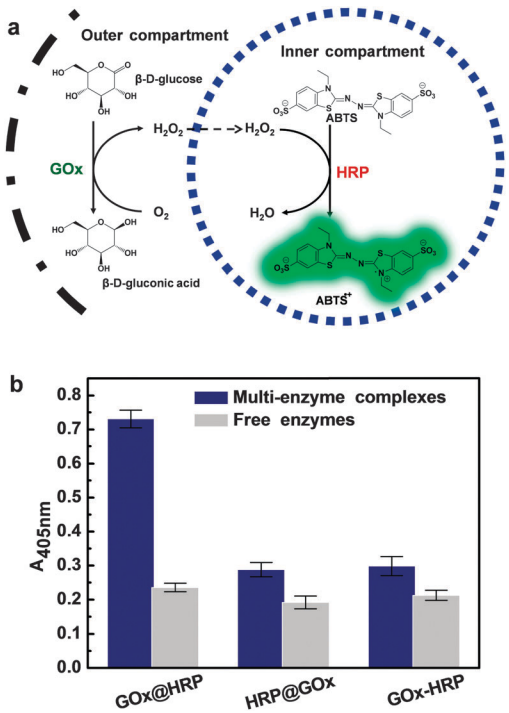

Fig. 2 Overall activities of the multi-enzyme incorporated complexes. (a) A schematic representation of the cascade reaction catalyzed by a GOx–HRP system; (b) comparison of overall activities of three types of multi-enzyme incorporated complexes (absorbance was measured after incubation for 10 min). The GOx and HRP contents in GOx@HRP, HRP@GOx and GOx–HRP were (2 wt%, 8 wt%), (8 wt%, 2 wt%) and (5 wt%, 5 wt%), respectively. The overall activities of multi-enzyme incorporated complexes were compared with the activities of free enzyme systems with the corresponding GOx and HRP contents.

transfer distance, and thus allows enzymes to exhibit a similar activity as their native counterparts.[20–30] In our study, the higher enzymatic activity compared to the native counterparts is due to the interaction between copper ions in nanocrystals and the incorporated metalloenzymes, mechanism for which has been well elaborated in our previous study.[18] More interesting, besides the effect of copper phosphate nanocrystals, the spatial distribution of the two enzymes has an obvious influence on the overall activity. GOx@HRP which has GOx on the outer shell and HRP in the core of the complex gave the highest overall activity, about 310% of activity compared to the free enzyme system.

As a demonstration, we applied GOx@HRP, which has the highest activity, for the convenient, sensitive detection of glucose in solution. The cascade reaction catalyzed by GOx@HRP produces $ABTS^{\bullet+}$ which is UV-Vis detectable. In a typical experiment, the absorbance at 405 nm was measured after 5 min of incubation of GOx@HRP in PBS solution containing glucose (0–100 μM) and ABTS (1 mM) at room temperature (Fig. S3a, ESI†). As shown in Fig. 3a, a good linearity between the absorbance and the concentration of glucose in the range of 0–20 μM was obtained ($R = 0.995$). The limit of detection (LOD) is 0.3 μM, lower than most of the reported colorimetric glucose sensors.[31–34] In addition, a direct visible detection of glucose can be achieved by using GOx@HRP (Fig. S3b, ESI†). In comparison, free enzymes, HRP@GOx and HRP–GOx produced less sensitive signals (Fig. S3c, ESI†). The long-term storage stability of enzymes was improved upon incorporation into the complexes. As shown in Fig. 3b the GOx@HRP retained ~90% initial activity after incubating in water solution at 25 °C for 7 days. In contrast, the free enzyme system in solution lost nearly 80% of the overall activity within 1 day. The enhanced enzyme stability is due to the confined configuration of the incorporated proteins, which prevents protein denaturation.[20–23] The almost unchanged activity of GOx@HRP also confirms that the enzyme-nanocrystal complex formed by co-precipitation and adsorption is very stable in water solution, without obvious the leakage of enzyme.

We propose that the highest performance of GOx@HRP is attributed to the ordered substrate transport on GOx@HRP in coherence with enzymatic cascade reactions. In the case of GOx@HRP, glucose and oxygen molecules first migrate to GOx on the shell while the product of the GOx-catalyzed reaction, H_2O_2, is subsequently directed to HRP in the core of the complexes. Substrate and intermediate concentration gradients help to drive and facilitate the GOx–HRP cascade, efficiently yielding a colored product. Especially, oxygen molecules that are needed for the first reaction are more accessible when GOx is located on the surface of the complexes. To confirm this, we studied the transport of the substrate and product molecules in the GOx@HRP catalyzed reactions (Fig. 4a) by confocal microscopy. By using the fluorescent glucose analogue 6-NBDG as an indicator, the uptake of the substrate by GOx@HRP was visualized as shown in Fig. 4b. The fluorescent glucose analogue was first captured by the complexes from solution due to the strong adsorption capability of the highly porous microspheres. Then the substrate molecules gradually diffused into the inside of microspheres (Fig. 4b and Movie S2, the video record can be found in the ESI†). By utilizing glucose as the substrate for GOx and Amplex Red as the substrate for HRP which can be converted to the highly fluorescent resorufin, we observed the generation of resorufin in the core of the complex where HRP is located, immediately after subjecting the substrates to GOx@HRP. As the enzymatic reaction proceeded, more resorufin molecules were generated and gradually diffused from the core to the bulk solution (Fig. 4c and Movie S3, the video record can be found in the ESI†).

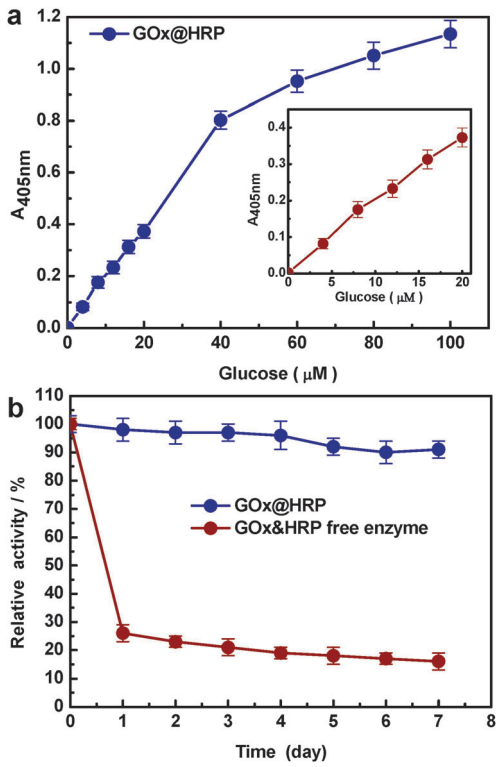

Fig. 3 Detection of glucose in solution. (a) Using GOx@HRP with the concentration of glucose in solution ranging from 0–100 μM and 0–20 μM (inset) (absorbance was measured after incubation for 5 min); (b) stability of GOx@HRP in aqueous solution at room temperature.

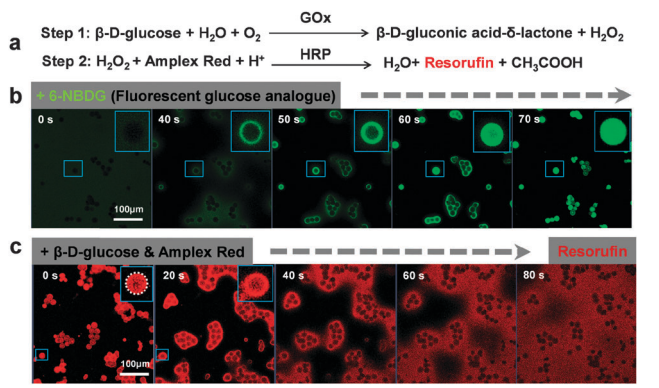

Fig. 4 Transport of substrates and products on GOx@HRP. (a) the cascade reaction catalysed by GOx and HRP using fluorescent substrates; (b) confocal images showing the transport of fluorescent glucose analogue 6-NBDG on GOx@HRP; (c) confocal images showing the transport of resorufin on GOx@HRP.

In summary, we presented a facile method that yields multi-enzyme–inorganic nanocrystal complexes with defined spatial localization of enzymes. Using GOx and HRP as model enzymes, we demonstrated that the high catalytic efficiency of the compartmentalized multi-enzyme systems is attributed to the directed substrate transport in coherence with enzymatic reactions. The ease of operation makes this method available for fabricating multi-enzyme systems with defined spatial distribution of enzymes so as to enable promising applications in biotechnology, diagnosis, biosensing and biomedical devices.

This work was supported by the National High Technology Research and Development Program (''863'' Program) of China under the grant number of 2014AA020507, the National Natural Science Foundation of China under the grant numbers 21036003 and 21206082, and the Tsinghua University Initiative Scientific Research Program under the grant number of 20131089191. We thank Prof. Richard N. Zare from Department of Chemistry, Stanford University for helpful discussions with this manuscript.

Notes and references

1 M. Marguet, C. Bonduelle and S. Lecommandoux, *Chem. Soc. Rev.*, 2013, **42**, 512.
2 M. M. Muthana, J. Y. Qu, Y. H. Li, L. Zhang, H. Yu, L. Ding, H. Malekan and X. Chen, *Chem. Commun.*, 2012, **48**, 2728.
3 G. F. Wang, H. Huang, B. J. Wang, X. J. Zhang and L. Wang, *Chem. Commun.*, 2012, **48**, 720.
4 O. Kreft, M. Prevot, H. Mohwald and G. B. Sukhorukov, *Angew. Chem., Int. Ed.*, 2007, **46**, 5605.
5 L. Zhang, J. F. Shi, Z. Y. Jiang, Y. J. Jiang, S. Z. Qiao, J. A. Li, R. Wang, R. J. Meng, Y. Y. Zhu and Y. Zheng, *Green Chem.*, 2011, **13**, 300.
6 K. Numajiri, M. Kimura, A. Kuzuya and M. Komiyama, *Chem. Commun.*, 2010, **46**, 5127.
7 M. Endo, Y. Y. Yang, T. Emura, K. Hidaka and H. Sugiyama, *Chem. Commun.*, 2011, **47**, 10743.
8 H. L. Zhang, J. Chao, D. Pan, H. J. Liu, Q. Huang and C. H. Fan, *Chem. Commun.*, 2012, **48**, 6405.
9 O. Idan and H. Hess, *ACS Nano*, 2013, **7**, 8658.
10 S. Schoffelen and J. C. M. van Hest, *Soft Matter*, 2012, **8**, 1736.
11 L. Bulow and K. Mosbach, *Trends Biotechnol.*, 1991, **9**, 226.
12 F. Verrier, S. O. An, A. M. Ferrie, H. Y. Sun, M. Kyoung, H. Y. Deng, Y. Fang and S. J. Benkovic, *Nat. Chem. Biol.*, 2011, **7**, 909.
13 J. L. Fu, M. H. Liu, Y. Liu, N. W. Woodbury and H. Yan, *J. Am. Chem. Soc.*, 2012, **134**, 5516.
14 R. Chandrawati, M. P. van Koeverden, H. Lomas and F. Caruso, *J. Phys. Chem. Lett.*, 2011, **2**, 2639.
15 R. Matsumoto, M. Kakuta, T. Sugiyama, Y. Goto, H. Sakai, Y. Tokita, T. Hatazawa, S. Tsujimura, O. Shirai and K. Kano, *Phys. Chem. Chem. Phys.*, 2010, **12**, 13904.
16 S. F. M. van Dongen, M. Nallani, J. L. L. M. Cornelissen, R. J. M. Nolte and J. C. M. van Hest, *Chem. – Eur. J.*, 2009, **15**, 1107.
17 Y. Liu, J. J. Du, M. Yan, M. Y. Lau, J. Hu, H. Han, O. O. Yang, S. Liang, W. Wei, H. Wang, J. M. Li, X. Y. Zhu, L. Q. Shi, W. Chen, C. Ji and Y. F. Lu, *Nat. Nanotechnol.*, 2013, **8**, 187.
18 J. Ge, J. Lei and R. N. Zare, *Nat. Nanotechnol.*, 2012, **7**, 428.
19 L. B. Wang, Y. C. Wang, R. He, A. Zhuang, X. P. Wang, J. Zeng and J. Hou, *J. Am. Chem. Soc.*, 2013, **135**, 1272.
20 J. Kim and J. W. Grate, *Nano Lett.*, 2003, **3**, 1219.
21 M. Yan, J. Ge, Z. Liu and P. Ouyang, *J. Am. Chem. Soc.*, 2006, **128**, 11008.
22 J. Ge, D. Lu, J. Wang and Z. Liu, *Biomacromolecules*, 2009, **10**, 1612.
23 J. Ge, D. Lu, J. Wang, M. Yan, Y. F. Lu and Z. Liu, *J. Phys. Chem. B*, 2008, **112**, 14319.
24 Y. Zhang, Q. Chen, J. Ge and Z. Liu, *Chem. Commun.*, 2013, **49**, 9815.
25 J. Zhu, Y. Zhang, D. Lu, R. N. Zare, J. Ge and Z. Liu, *Chem. Commun.*, 2013, **49**, 6090.
26 Y. Zhang, Y. Dai, M. Hou, T. Li, J. Ge and Z. Liu, *RSC Adv.*, 2013, **3**, 22963.
27 J. Ge, D. Lu, Z. Liu and Z. Liu, *Biochem. Eng. J.*, 2009, **44**, 53.
28 J. Ge, C. Yang, J. Zhu, D. Lu and Z. Liu, *Top. Catal.*, 2012, **55**, 1070.
29 Z. Li, Y. Zhang, M. Lin, P. Ouyang, J. Ge and Z. Liu, *Org. Process Res. Dev.*, 2013, **17**, 1179.
30 R. Wang, Y. Zhang, J. Huang, D. Lu, J. Ge and Z. Liu, *Green Chem.*, 2013, **15**, 1155.
31 H. Wei and E. Wang, *Anal. Chem.*, 2008, **80**, 2250.
32 J. S. Mu, Y. Wang, M. Zhao and L. Zhang, *Chem. Commun.*, 2012, **48**, 2540.
33 M. Ornatska, E. Sharpe, D. Andreescu and S. Andreescu, *Anal. Chem.*, 2011, **83**, 4273.
34 Y. J. Song, K. G. Qu, C. Zhao, J. S. Ren and X. G. Qu, *Adv. Mater.*, 2010, **22**, 2206.

